



HAL
open science

Ferromagnetism in novel compounds of the $R_3Pt_23Si_{11}$ series with heavy rare earth: Gd, Tb, Dy, Ho and Er

Christine Opagiste, Rose-Marie Galéra

► To cite this version:

Christine Opagiste, Rose-Marie Galéra. Ferromagnetism in novel compounds of the $R_3Pt_23Si_{11}$ series with heavy rare earth: Gd, Tb, Dy, Ho and Er. *Journal of Magnetism and Magnetic Materials*, 2014, 357, pp.13 - 17. 10.1016/j.jmmm.2014.01.010 . hal-00940502

HAL Id: hal-00940502

<https://hal.science/hal-00940502>

Submitted on 1 Feb 2014

HAL is a multi-disciplinary open access archive for the deposit and dissemination of scientific research documents, whether they are published or not. The documents may come from teaching and research institutions in France or abroad, or from public or private research centers.

L'archive ouverte pluridisciplinaire **HAL**, est destinée au dépôt et à la diffusion de documents scientifiques de niveau recherche, publiés ou non, émanant des établissements d'enseignement et de recherche français ou étrangers, des laboratoires publics ou privés.

Ferromagnetism in novel compounds of the $R_3Pt_{23}Si_{11}$ series with heavy rare earth: Gd, Tb, Dy, Ho and Er

C. Opagiste^{a,b,1}, R. M. Galéra^{a,b}

^a*Univ. Grenoble Alpes, Inst NEEL, F-38042 Grenoble, France*

^b*CNRS, Inst NEEL, F-38042 Grenoble, France*

Abstract

We have synthesized new compounds of the $R_3Pt_{23}Si_{11}$ series with $R=Gd, Tb, Dy, Ho$ and Er , and studied their magnetic and thermodynamic properties. X-ray powder diffraction characterization confirms that all these compounds crystallize in the same face-centered cubic structure, space group $Fm\bar{3}m$, as $Ce_3Pt_{23}Si_{11}$. They all present a ferromagnetic order at low temperatures. The Curie temperatures range between 42 ± 1 K to 3.39 ± 0.05 K for $Gd_3Pt_{23}Si_{11}$ and $Er_3Pt_{23}Si_{11}$ respectively. For all compounds the value of the spontaneous moment at 2 K is far below the value expected for the saturated moment of the R^{3+} ions, except for the Gd compound. The estimations of the magnetic entropy at T_C remain smaller than the full entropy of the fundamental multiplet, $R \ln(2J + 1)$. Both reductions, of the moment and of the magnetic entropy, are ascribed to the crystal field effects. In the paramagnetic phase the thermal variation of the susceptibilities follow a Curie-Weiss law with Curie constants in good agreement with the theoretical values

Keywords: rare-earth intermetallics ferromagnetism heat-capacity entropy

1. Introduction

The ternary Ce-Pt-Si phase diagram has been the focus of great interest due to the discovery of the non-centrosymmetric heavy fermion superconductor $CePt_3Si$ [1]. In the course of the study of this Ce-Pt-Si ternary system,

¹christine.opagiste@grenoble.cnrs.fr

Gribanov *et al.* have reported for the first time the existence of a defined cubic compound with the composition $\text{Ce}_3\text{Pt}_{23}\text{Si}_{11}$ that can be found in equilibrium in the cerium deficient CePt_3Si compound [2].

We recently started the investigation of the new series $\text{R}_3\text{Pt}_{23}\text{Si}_{11}$ with R a light rare earth element (Ce, Pr and Nd) [3, 4, 5, 6]. Our studies on a very high quality single crystal of $\text{Ce}_3\text{Pt}_{23}\text{Si}_{11}$ have revealed that a ferromagnetic order is stabilised at $T_c = 0.44$ K. In the ferromagnetic phase, a weak but significant magnetic anisotropy exists with an easy magnetization axis along the threefold axes of the cube. In the paramagnetic phase, the magnetic susceptibility follows a Curie-Weiss law, fully consistent with a normal trivalent Ce^{3+} ion. However, the observation by neutron spectroscopy of two inelastic lines of magnetic origin remains an intriguing point that is still not understood [3, 4]. In the same series we have synthesized the novel compounds with Pr and Nd. Our studies on polycrystalline samples show that at low temperatures $\text{Pr}_3\text{Pt}_{23}\text{Si}_{11}$ becomes a Van Vleck type paramagnetic due to a non magnetic crystalline electric field ground state and that the magnetization of $\text{Nd}_3\text{Pt}_{23}\text{Si}_{11}$ has a metamagnetic behaviour [5, 6].

To our knowledge on the side of the heavy rare earth elements, except $\text{Yb}_3\text{Pt}_{23}\text{Si}_{11}$ [7], no other compound has been synthesized and studied up to now. Quite recently we have successfully synthesized five new compounds in the $\text{R}_3\text{Pt}_{23}\text{Si}_{11}$ series with Gd, Tb, Dy, Ho and Er. In this paper, we report investigations of the crystallographic structure, magnetic behaviour and heat capacity properties of these compounds in the temperature range 2-300 K.

2. Samples synthesis and crystallographic studies

High quality polycrystalline samples of $\text{R}_3\text{Pt}_{23}\text{Si}_{11}$ have been prepared in an induction furnace. Stoichiometric proportions of the different constituents; R= Gd, Tb, Dy, Ho and Er (99.9%, Johnson Matthey), Pt (99.95%, Alfa Aesar) and Si (99.9999%, Alfa Aesar), were melted in a water cooled copper crucible under a highly-purified argon atmosphere. The samples were melted several times to improve the homogeneity. Mass losses during this step were less than 0.6%. No further heat treatment was applied.

The crystal structure and the sample quality were checked by conventional X-ray powder diffraction (Cu-K α radiation on a Philips PW1730 diffractometer), whilst structural refinements were performed using the FullProf program [8]. The results of the refinements are fully consistent with the fcc crystal structure ($Fm\bar{3}m$ space group) already reported for $\text{Ce}_3\text{Pt}_{23}\text{Si}_{11}$ [9]. Figure 1

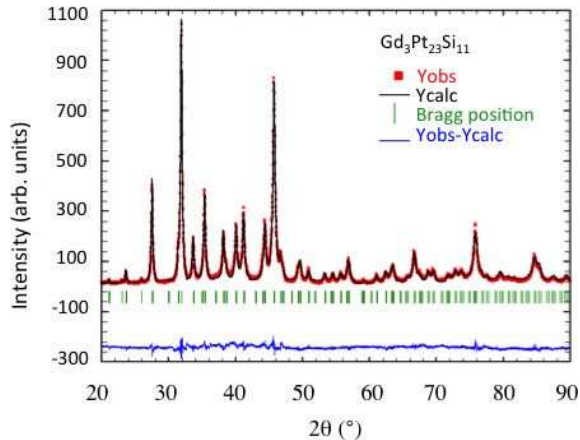


Figure 1: (Color online) X-ray diffraction pattern of $\text{Gd}_3\text{Pt}_{23}\text{Si}_{11}$ with the results of the FullProf refinements.

compares the experimental X-ray diffraction pattern to the simulated one for $\text{Gd}_3\text{Pt}_{23}\text{Si}_{11}$. Within the experimental resolution no impurity phase is observed in the Gd-, Tb- and $\text{Ho}_3\text{Pt}_{23}\text{Si}_{11}$ samples. In the $\text{Dy}_3\text{Pt}_{23}\text{Si}_{11}$ and $\text{Er}_3\text{Pt}_{23}\text{Si}_{11}$ samples the presence of a weak amount ($\approx 5\%$) of the Pt_2Si phase is detected. The values of the refined lattice parameter, a , at room temperature and the details of the Rietveld refinements are reported in table 1. The atomic coordinates in the elementary cell are summarized in tables 2 to 6 for each compound. The variation of the lattice parameter with the atomic number of the rare earth elements is reported in figure 2. The decrease of the lattice parameter with the atomic number is consistent with the effect of the lanthanide contraction.

3. Magnetic Properties

Magnetization measurements were performed on polycrystalline samples using different magnetometers based on the extraction method in the temperature range 2-300 K. We used a commercial Quantum Design MPMS magnetometer for measurements in fields up to 5 T and a second experimental set-up, equipped with resistive detection coils in fields up to 8 T. The thermal variation of the magnetization under an applied field of 100 Oe has been measured between 2 and 300 K for Dy- Ho- and $\text{Er}_3\text{Pt}_{23}\text{Si}_{11}$. For each compound, below a certain temperature the thermal variation presents a step increase and remains constant down to 2 K. This is illustrated, for

Table 1: Crystallographic details and results of the FullProf refinements realized assuming a cubic structure of the $\text{Ce}_3\text{Pt}_{23}\text{Si}_{11}$ type: space group $Fm\bar{3}m$ (n° 225) and $Z=8$. Column 4 gives the number of measured reflections. For all compounds the same 28 parameters have been refined. * presence of $\approx 5\%$ of the phase Pt_2Si .

Compound	a(Å)	D_{cal} (g/cm ³)	Reflexions	χ^2
$\text{Gd}_3\text{Pt}_{23}\text{Si}_{11}$	16.8249(7)	14.693	296	5.88
$\text{Tb}_3\text{Pt}_{23}\text{Si}_{11}$	16.8181(8)	14.725	286	5.82
$\text{Dy}_3\text{Pt}_{23}\text{Si}_{11}^*$	16.814(1)	14.767	299	7.41
$\text{Ho}_3\text{Pt}_{23}\text{Si}_{11}$	16.8015(5)	14.820	272	7.92
$\text{Er}_3\text{Pt}_{23}\text{Si}_{11}^*$	16.7979(5)	14.849	283	5.92

Table 2: Atomic coordinates and isotropic displacement parameters for $\text{Gd}_3\text{Pt}_{23}\text{Si}_{11}$.

Atom	Wyckoff site	x/a	y/b	z/c	U_{iso} (Å ²)	Occupation
Gd	24 <i>d</i>	0	1/4	1/4	1.2	1
Pt ₁	32 <i>f</i>	0.0808(1)	0.0808(1)	0.0808(1)	1.0	1
Pt ₂	32 <i>f</i>	0.3088(1)	0.3088(1)	0.3088(1)	0.8	1
Pt ₃	24 <i>e</i>	0.3745(2)	0	0	0.5	1
Pt ₄	96 <i>k</i>	0.0848(1)	0.0848(1)	0.2525(1)	0.9	1
Si ₁	24 <i>e</i>	0.188(1)	0	0	1.0	1
Si ₂	32 <i>f</i>	0.1723(6)	0.1723(6)	0.1723(6)	1.0	1
Si ₃	32 <i>f</i>	0.3889(8)	0.3889(8)	0.3889(8)	1.5	1

Table 3: Atomic coordinates and isotropic displacement parameters for $\text{Tb}_3\text{Pt}_{23}\text{Si}_{11}$.

Atom	Wyckoff site	x/a	y/b	z/c	U_{iso} (Å ²)	Occupation
Tb	24 <i>d</i>	0	1/4	1/4	1.0	1
Pt ₁	32 <i>f</i>	0.0826(2)	0.0826(2)	0.0826(2)	1.2	1
Pt ₂	32 <i>f</i>	0.3093(1)	0.3093(1)	0.3093(1)	0.4	1
Pt ₃	24 <i>e</i>	0.3738(3)	0	0	0.4	1
Pt ₄	96 <i>k</i>	0.0847(1)	0.0847(1)	0.2524(1)	0.7	1
Si ₁	24 <i>e</i>	0.184(2)	0	0	1.5	1
Si ₂	32 <i>f</i>	0.1759(8)	0.1759(8)	0.1759(8)	1.5	1
Si ₃	32 <i>f</i>	0.3918(8)	0.3918(8)	0.3918(8)	1.5	1

Table 4: Atomic coordinates and isotropic displacement parameters for Dy₃Pt₂₃Si₁₁.

Atom	Wyckoff site	x/a	y/b	z/c	U_{iso} (Å ²)	Occupation
Dy	24 <i>d</i>	0	1/4	1/4	1.0	1
Pt ₁	32 <i>f</i>	0.0828(2)	0.0828(2)	0.0828(2)	1.5	1
Pt ₂	32 <i>f</i>	0.3089(2)	0.3089(2)	0.3089(2)	0.8	1
Pt ₃	24 <i>e</i>	0.3753(4)	0	0	1.1	1
Pt ₄	96 <i>k</i>	0.0850(1)	0.0850(1)	0.2527(1)	0.8	1
Si ₁	24 <i>e</i>	0.194(2)	0	0	1.5	1
Si ₂	32 <i>f</i>	0.170(1)	0.170(1)	0.170(1)	1.5	1
Si ₃	32 <i>f</i>	0.386(1)	0.386(1)	0.386(1)	1.5	1

Table 5: Atomic coordinates and isotropic displacement parameters for Ho₃Pt₂₃Si₁₁.

Atom	Wyckoff site	x/a	y/b	z/c	U_{iso} (Å ²)	Occupation
Ho	24 <i>d</i>	0	1/4	1/4	1.3	1
Pt ₁	32 <i>f</i>	0.0829(2)	0.0829(2)	0.0829(2)	0.7	1
Pt ₂	32 <i>f</i>	0.3093(1)	0.3093(1)	0.3093(1)	0.2	1
Pt ₃	24 <i>e</i>	0.3770(3)	0	0	0.4	1
Pt ₄	96 <i>k</i>	0.0848(1)	0.0848(1)	0.2524(1)	0.8	1
Si ₁	24 <i>e</i>	0.182(2)	0	0	1.5	1
Si ₂	32 <i>f</i>	0.1711(8)	0.1711(8)	0.1711(8)	1.5	1
Si ₃	32 <i>f</i>	0.388(1)	0.388(1)	0.388(1)	1.5	1

Table 6: Atomic coordinates and isotropic displacement parameters for Er₃Pt₂₃Si₁₁.

Atom	Wyckoff site	x/a	y/b	z/c	U_{iso} (Å ²)	Occupation
Er	24 <i>d</i>	0	1/4	1/4	0.9	1
Pt ₁	32 <i>f</i>	0.0829(2)	0.0829(2)	0.0829(2)	1.2	1
Pt ₂	32 <i>f</i>	0.3081(1)	0.3081(1)	0.3081(1)	0.8	1
Pt ₃	24 <i>e</i>	0.3747(3)	0	0	0.8	1
Pt ₄	96 <i>k</i>	0.0849(1)	0.0849(1)	0.2525(1)	0.9	1
Si ₁	24 <i>e</i>	0.190(2)	0	0	1.6	1
Si ₂	32 <i>f</i>	0.1653(8)	0.1653(8)	0.1653(8)	1.6	1
Si ₃	32 <i>f</i>	0.3897(8)	0.3897(8)	0.3897(8)	1.6	1

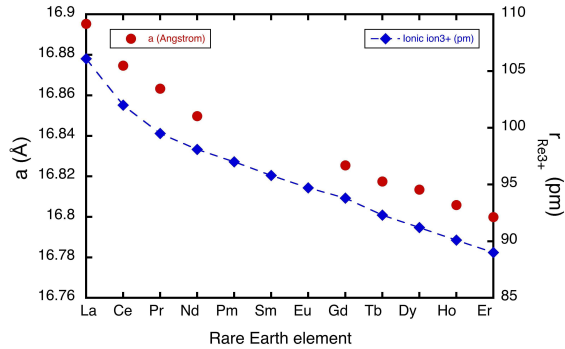


Figure 2: (Color online) Comparison between the variation of the lattice parameter and the ionic radius of the trivalent rare earth ion in the $R_3Pt_{23}Si_{11}$ series. The dashed line is a guide for the eyes.

example, in figure 3 for the $Ho_3Pt_{23}Si_{11}$ and $Er_3Pt_{23}Si_{11}$ compounds. Such a behavior is characteristic of a transition into a ferromagnetic phase. The values of the Curie temperatures deduced from these measurements are given in table 7.

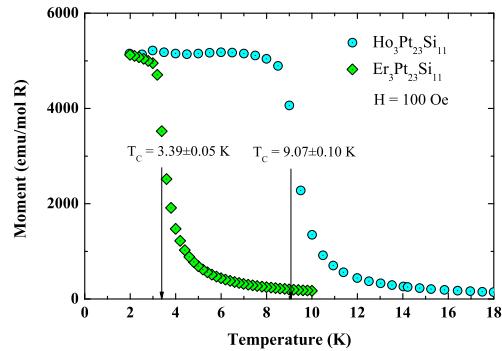


Figure 3: (Color online) Thermal variation of the moment in $Ho_3Pt_{23}Si_{11}$ and $Er_3Pt_{23}Si_{11}$ measured under an applied field of 100 Oe. The step increase at 3.39 and 9.07 K is the signature of the ferromagnetic transition in $Er_3Pt_{23}Si_{11}$ and $Ho_3Pt_{23}Si_{11}$ respectively.

In the paramagnetic phase, isothermal magnetization curves $M(H)$ have been measured up to 300K. The inverse of the magnetic susceptibility is deduced from the Arrott plots [10]: $M^2 = f(H/M)$. For all compounds $\frac{1}{\chi}$ varies

Table 7: The Curie temperatures T_C deduced from the magnetic and heat capacity measurements are reported in column 2 and 3 respectively. C_{th} is the Curie constant of the trivalent rare earth ion in emu.K per mol of R ion (emu.K/mol R). n_{ex} is the value of the exchange constant used in the calculation of the Curie-Weiss law : $\frac{1}{\chi} = \frac{T}{C_{th}} - n_{ex}$. Columns 6 and 7 give the saturation magnetic moment and the spontaneous magnetization at 2 K respectively.

	T_C^{mag} (K)	T_C^{HC} (K)	C_{th}	n_{ex}	$g_J J$ (μ_B)	M_s (μ_B/R)
Gd ₃ Pt ₂₃ Si ₁₁	42±1	40.82±0.05	7.87	5.8	7	7.00±0.10
Tb ₃ Pt ₂₃ Si ₁₁	25±1	23.77±0.05	11.65	2.2	9	5.86±0.10
Dy ₃ Pt ₂₃ Si ₁₁	15.99±0.10	16.03±0.05	14.17	1.2	10	7.08±0.10
Ho ₃ Pt ₂₃ Si ₁₁	9.07±0.10	9.13±0.10	14.06	0.6	10	7.06±0.19
Er ₃ Pt ₂₃ Si ₁₁	3.39±0.05	3.30±0.05	11.47	0.28	9	4.79±0.23

linearly with the temperature as shown in figure 4. The lines in figure 4 represent the Curie-Weiss law : $\frac{1}{\chi} = \frac{T}{C_{th}} - n_{ex}$, with C_{th} the theoretical Curie constant of the trivalent rare earth ion and n_{ex} the exchange constant (see table 7). Theoretically $n_{ex} = \frac{\theta_p}{C_{th}}$, with θ_p is the paramagnetic Curie temperature.

In the ferromagnetic phase the magnetization curves have been measured down to 2 K, the base temperature of the experimental setups. The magnetization curves for Gd₃Pt₂₃Si₁₁, Tb₃Pt₂₃Si₁₁ and Dy₃Pt₂₃Si₁₁ are reported in figure 5 together with the thermal variation of the spontaneous moment. The value of the spontaneous moment is deduced from the Arrott's plots. At 2 K the spontaneous moment is found systematically smaller than the expected value $M_S(0 \text{ K}) = g_J J$ for all the compounds except for Gd₃Pt₂₃Si₁₁ (see table 7). In this last compound the expected 7 μ_B/Gd for a S=7/2 ion are found (see figure 5). From the values observed at 2 K for the spontaneous magnetization of all the other compounds it is obvious that the saturation of the magnetic moment is not reached at zero K. This reduction of the magnetic moment is ascribed to the crystalline electric field (CEF) effects that in crystals partly lift the degeneracy of the fundamental multiplet. Note that, contrary to the light rare earth compounds [4, 5], the magnetic susceptibility shows no deviation to the Curie-Weiss law at low temperatures in the heavy rare earth side of the series (see figure 4). This deviation is also a CEF effect associated with the population of the excited levels as the temperature increases. It gets rapidly reduced as soon as the excited CEF levels become

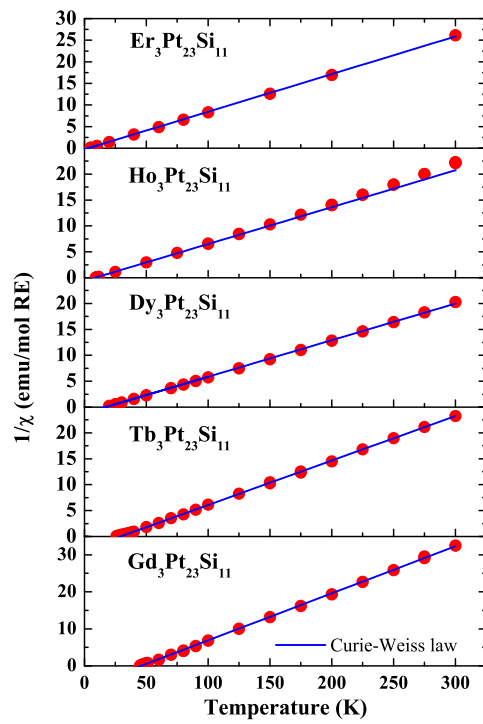


Figure 4: (Color online) Thermal variation of the inverse of the susceptibility of the five studied compounds.

closer in energy. This is likely the case for the heavy rare earth compounds owing to the high degeneracy of the $J=L+S$ multiplet of heavy rare earth ions. The evolution of the Curie temperature with the rare earth ion in the series is compared with that of the de Gennes factor in figure 6. A very good consistency is observed between both evolutions in the whole series.

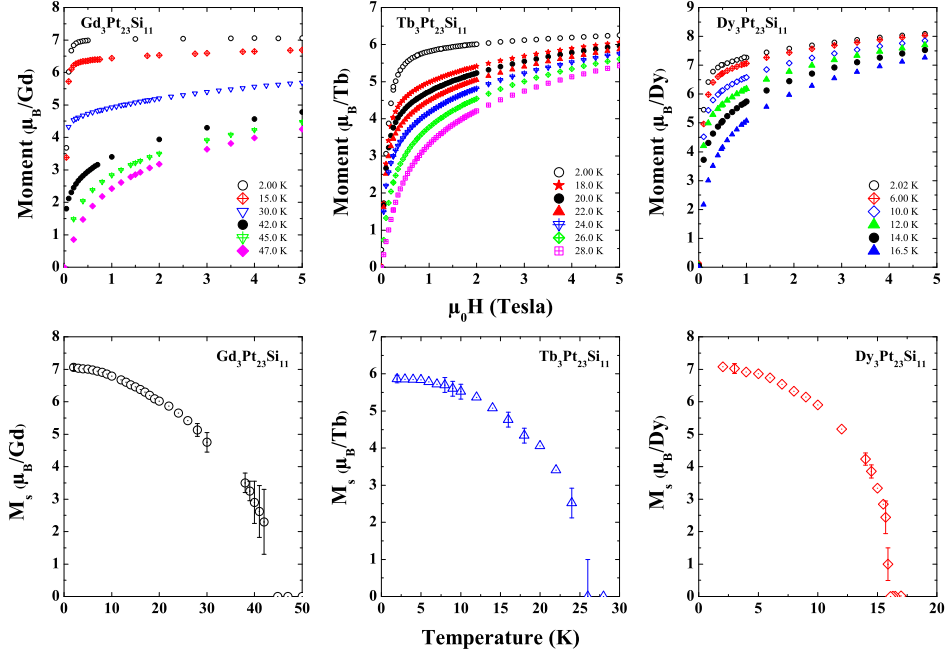


Figure 5: (Color online) Upper part magnetization curves measured on $Gd_3Pt_{23}Si_{11}$, $Tb_3Pt_{23}Si_{11}$ and $Dy_3Pt_{23}Si_{11}$ respectively at different temperatures below and above T_C . Lower part thermal variation of the spontaneous magnetization for $Gd_3Pt_{23}Si_{11}$, $Tb_3Pt_{23}Si_{11}$ and $Dy_3Pt_{23}Si_{11}$ respectively.

4. Thermodynamic properties: heat capacity, entropy

In the temperature range 1.9 - 300K, the heat capacity was measured using the relaxation method with a commercial Quantum Design PPMS. The measurements were focused at low temperature in order to determine

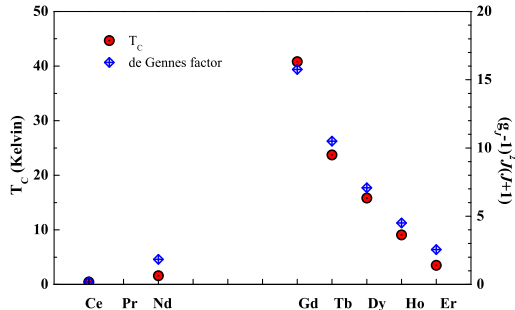


Figure 6: (Color online) Comparison of the evolution with the rare earth ion between the Curie temperature (dots) and the de Gennes factor (diamonds) [11] in the $R_3Pt_{23}Si_{11}$ series. Note that the Pr compound behaves as a Van Vleck paramagnet at low temperature [5].

precisely the temperature of the ferromagnetic transition. For all the compounds a clear lambda anomaly is observed at T_C as shown for instance in figure 7 for the specific heat of $Er_3Pt_{23}Si_{11}$ and $Dy_3Pt_{23}Si_{11}$. The Curie temperatures deduced from the inflexion point of the lambda anomaly are reported in table 7. The values are consistent with those determined from the magnetic measurements.

A tentative determination of the magnetic entropy from the experimental specific heat has been performed for all the compounds. This is done with the aim to determine the degeneracy of the magnetic ground state. As stated above it is expected that the CEF interactions partly lift the $2J + 1$ degeneracy of the fundamental multiplet. The Curie temperature of some compounds is relatively high. Thus, it is necessary to subtract properly the phonon contribution to the total specific heat in order to get the magnetic contribution C_{mag} . For these compounds the phonon contribution is determined from the specific heat curve measured in the non magnetic $La_3Pt_{23}Si_{11}$ compound [4] after normalizing the temperature by the factor $F = \sqrt[3]{\frac{\theta_D(R_3Pt_{23}Si_{11})}{\theta_D(La_3Pt_{23}Si_{11})}}$, where θ_D is the Debye temperature of the compound [12]. For instance, in figure 7 the total specific heat of $Dy_3Pt_{23}Si_{11}$ is reported with the phonon contribution deduced from the $La_3Pt_{23}Si_{11}$ specific heat.

Figure 8 gathers the thermal variation of the estimated magnetic entropy of all the studied compounds. At the Curie temperature, the entropy for $Gd_3Pt_{23}Si_{11}$ reaches only 92.6% of $3 \times R \ln 8$, the expected value for a $S=7/2$

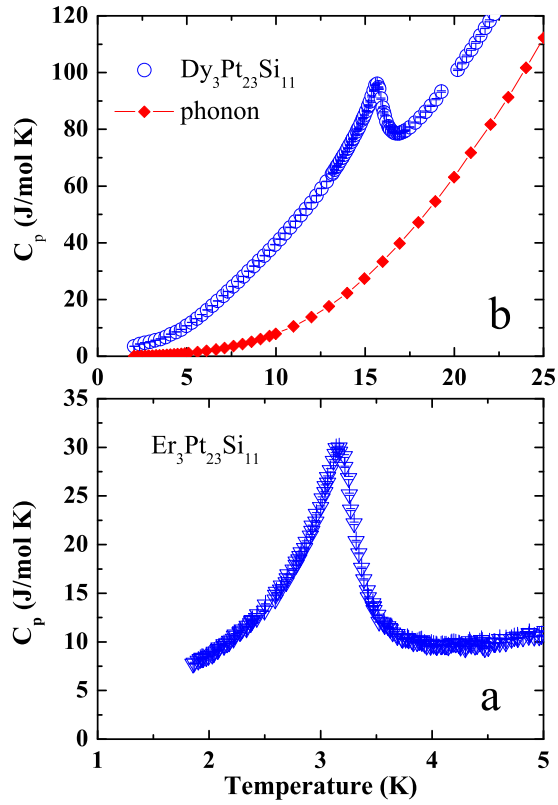


Figure 7: (Color online) a) Thermal variation of the specific heat in $\text{Er}_3\text{Pt}_{23}\text{Si}_{11}$ in the low temperature range. The Curie temperature T_C is deduced from the inflexion point of the lambda anomaly. b) Thermal variation of the total specific heat in $\text{Dy}_3\text{Pt}_{23}\text{Si}_{11}$ (open dots) and of the phonon contribution deduced from the $\text{La}_3\text{Pt}_{23}\text{Si}_{11}$ measurements (full squares)(see text).

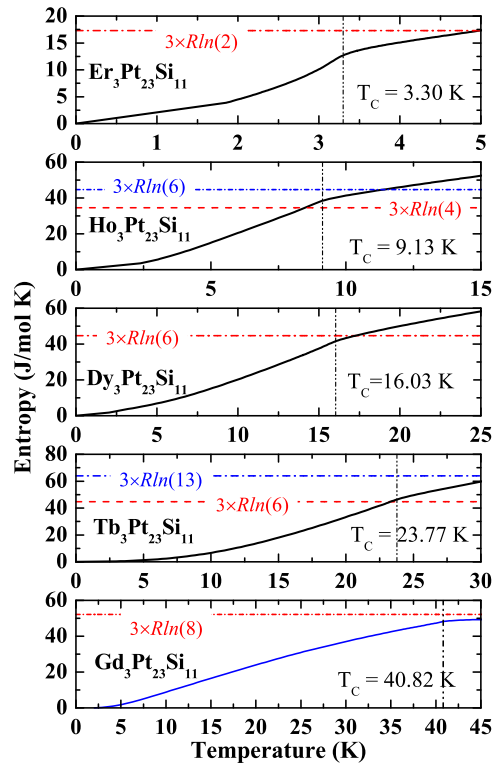


Figure 8: (Color online) Thermal evolution of the estimated magnetic entropy in Gd-, Tb-, Dy-, Ho-, $\text{Er}_3\text{Pt}_{23}\text{Si}_{11}$.

ion. The magnetic entropy is obtained by integrating $\frac{C_{mag}}{T}$ from 0 K to T. As the lowest temperature reached in the present measurements is only 1.9 K, it is likely that the magnetic entropy is underestimated. Nonetheless for the other compounds the entropy at T_C reaches values far lower than the $3 \times R \ln(2J + 1)$ upper limits. According to the magnetic measurements, this reduction is likely due the CEF effects.

5. Conclusion

In the present study we show that compounds of the $R_3Pt_{23}Si_{11}$ series exist with Gd, Tb, Dy, Ho and Er. This proves the high stability of this ternary series. The magnetic studies show that, all compounds follow a Curie-Weiss law and that a ferromagnetic order is stabilized at low temperatures. As expected in a scenario of normal RKKY-type exchange interactions, the highest value of T_C is found in the Gd compound. It is also observed that in the series the evolution of the values of T_C or T_N (case of $Nd_3Pt_{23}Si_{11}$) with the atomic number of the rare earth ion is in a fair agreement with the de Gennes law. Though no deviation to the Curie-Weiss law is observed at low temperature on the magnetic susceptibility, the reduced values of the spontaneous magnetization together with a magnetic entropy at T_C smaller than $3 \times R \ln(2J + 1)$, are consistent with the lifting of the multiplet degeneracy by the crystalline electric field effects in the Tb, Dy, Ho and Er compounds.

Acknowledgments

We are grateful to R. Haettel, A. Hadj-Azzem, J. Balay, Y. Deschanel, E. Eyraud, D. Dufeu and P. Lachkar from the Institut Néel, for their technical assistance.

References

- [1] E. Bauer, G. Hilscher, H. Michor, C. Paul, E. W. Scheidt, A. Griбанov, Y. Seropegin, H. Noël, M. Sigrist, P. Rogl, Phys. Rev. Lett. 92 (2004) 027003.
- [2] A. V. Griбанov, Y. D. Seropegin, A. I. Tursina, O. I. Bodak, P. Rogl, H. Noel, J. Alloys Compd. 383 (1-2) (2004) 286 – 289.
- [3] C. Opagiste, C. Paulsen, E. Lhotel, P. Rodiere, R.-M. Galera, P. Bordet, P. Lejay, J. Magn. Mater. 321 (6) (2009) 613 – 618.

- [4] C. Opagiste, R.-M. Galéra, M. Amara, C. Paulsen, S. Rols, B. Ouladdiaf, *Phys. Rev. B* 84 (2011) 134401.
- [5] C. Opagiste, R.-M. Galéra, *Journal of Alloys and Compounds* 541 (2012) 403 – 406.
- [6] C. Opagiste, M. Jackson, R.-M. Galéra, E. Lhotel, C. Paulsen, B. Ouladdiaf, *Journal of Magnetism and Magnetic Materials* 340 (2013) 46 – 49.
- [7] D. Kaczorowski, A. Griбанov, S. Safronov, P. Rogl, Y. Seropegin, *Journal of Alloys and Compounds* 509 (37) (2011) 8987 – 8990.
- [8] J. Rodriguez-Carvajal, *Satellite Meeting on Powder Diffraction of the XV Congress of the IUCr, Book of Abstracts*, 1990.
- [9] A. I. Tursina, A. V. Griбанov, Y. D. Seropegin, K. V. Kuyukov, O. I. Bodak, *J. Alloys Compd.* 347 (1-2) (2002) 121 – 123.
- [10] A. Arrott, *Phys. Rev.* 108 (1957) 1394.
- [11] P.-G. de Gennes, *Comptes Rendus de l'Académie des Sciences* 247 (1959) 1836.
- [12] M. Bouvier, P. Lethuillier, D. Schmitt, *Phys. Rev. B* 43 (16) (1991) 13137–13144.